Isolated Swiss-Forward Three-Phase Rectifier for Aircraft Applications

Marcelo Silva, Nico Hensgens, Jesús Oliver, Pedro Alou, Óscar García, and José A Cobos

Abstract—Recently an important increase of the electrical equipment in modern aircrafts is leading to an increase in the demand for electrical power. The usual electrical power distribution in aircraft applications is done via a three-phase 115Vac grid. A new trend of DC distribution is emerging employing a 270 Vdc grid. This yields the need for high-efficiency and high power-density AC-DC converters, connecting the two grids while providing galvanic isolation. Traditionally 12-pulse autotransformer passive rectifiers are used in aircraft applications. This converter is robust and highly reliable, however it is a non-controlled topology and it is relatively heavy because of the low frequency power transformer. Two-stage rectifier system approaches, employing three-phase PWM rectifiers or active filters and isolated DC-DC converters, are good alternatives to be applied in aircraft applications, to reduce the weight by using high frequency transformers and inductors. However, two-stage topologies process the energy twice leading to lower efficiency, power density. The reliability is also not very high due to a high semiconductor component count.

This paper presents a new isolated single-stage PWM rectifier system, based on the recently presented non-isolated Swiss recti-fier topology, called the Swiss-Forward rectifier. The principle of operation of this converter topology is presented together with detailed design guidelines and experimental validation on a 3.3kW 115Vac to 270Vdc prototype.
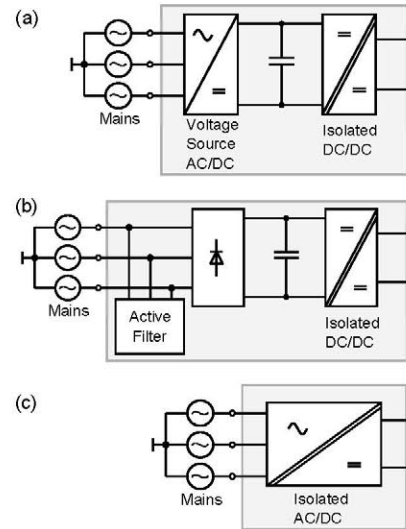
Figure 1.   (a) Two-Stage rectifier system. (b) three-phase rectifier with active filter plus isolated DC-DC converter topology, (c) single-stage isolated AC-DC converter

I. INTRODUCTION

In recent years, the topic of the More Electric Aircraft (MEA) has become important [1]–[3]. This term describes the trend to replace more and more systems in modern and future aircrafts, which have previously been hydraulic or pneumatic, by electrical systems. This increases the electric power demand in these aircrafts leading to a need for compact and efficient power converters for aircraft applications and a resulting research focus in this area [4]. The electric power distribution in aircrafts is normally done via two separate grids, one three-phase AC grid with 115V and either fixed grid frequency of 400Hz, or in some cases variable grid frequency between 320-800Hz, the second grid is a 28Vdc grid. However in recent developments the possibility of employing a 270Vdc grid has been investigated, leading to lower weight in the wiring. The power generation is normally done via only one single type of generator feeding the 115Vac 3-phase grid. For all the equipment not being supplied in this way, power converters are needed to provide the correct voltage levels for all loads. Since the use of a 270Vdc grid is very new, no 270Vdc generators are yet in use in modern aircrafts, and power converters need to be used to convert the available 115V three-phase AC voltage into a 270Vdc voltage. This work is focused on the design of isolated rectifier systems from 115Vac to 270Vdc for aircraft applications.

The easiest approach to convert from the three-phase AC to DC voltage is by employing a simple diode-bridge. However this results in current shapes which are not sinusoidal and thus a high total harmonic distortion (THD) [5] leading to additional losses in the cabling and possible problems in other equipment. Additionally a simple diode-bridge does not provide isolation between the AC and DC grids.

The classical approach in aircraft applications to obtain low THD is by using the 12-pulse autotransformer passive recti-fiers. this is a simple converter without any transistor, leading to highly robust and reliable systems [6], [7]. However it is a non-controlled topology and it is relatively heavy because of the low frequency power transformer. Another widely used approach to obtain low THD, good power factor (PF), and isolation is the use of a two-stage topology (cf. Fig. 1a), consisting of a three-phase PWM rectifier providing high PF and low THD and an additional DC-DC converter providing isolation. This approach allows to divide the problem and optimize the system separately, focusing the rectifier design on the AC steady state performance (PF and THD) and leave the dynamic requirements to the DC-DC converter [8]. The main disadvantage of this approach is that the whole power has to be processed twice, once by the PWM rectifier and once by the DC-DC converter, leading to high losses and thus low efficiency. Additionally, the number of semiconductors is
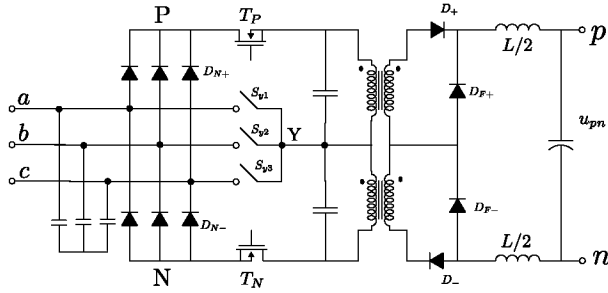
Figure 2. Topology schematic of the proposed Swiss-Forward converter

high leading to lower reliability and the power density of the two-stage converter is also expected not to be very good. An alternative is replacing the PWM rectifier by a diode-bridge with active power filter (cf. Fig. 1b). The active filter only needs to process a small part of the total power. In this way the global efficiency and power-density can be increased, however the number of semiconductors still remains high.

In order to obtain high efficiency, high power density and high reliability (i.e. a low number of semiconductors), the use of a single-stage topology is advantageous (cf. Fig. 1c). In [9] an isolated single-stage topology has been presented based on a two-switch three-phase rectifier [10]. This converter is relatively easy to control because it operates in discontinuous conduction mode (DCM) and it can be used at high switching frequencies due to ZVS. However, at the power levels considered in this work (3.3kW), DCM converters are not appropriate because of the high RMS currents in the semiconductors, inductors and the transformer. In [11] and [12] two different isolated buck-type quasi-single-stage three-phase converter have been proposed, however, despite it being a quasi-single-stage converter, the number of semiconductors is very high.

In [13], [14] a new type of rectifier is proposed, called the Swiss Rectifier (SR), consisting of a diode-bridge and three bidirectional switches, and two in the topology integrated buck-type DC-DC converters. It is possible to replace the buck-converters by other types of DC-DC converters including isolated DC-DC converters and thus obtaining an isolated quasi-single-stage topology.

In this paper, a SR-derived quasi-single-stage isolated three-phase rectifier is presented, called the Swiss-Forward Rectifier. The paper explains the principle of operation of the converter, including a method of demagnetizing the transformer using a resonant reset technique, as well as the design of a demonstrator prototype with a power rating of 3.3 kW and a switching frequency of 100kHz.

II. SWISS FORWARD RECTIFIER

The Swiss Rectifier is a new topology presented in [13], [14]. It is a buck-type topology which is also called current source converter. As shown in these papers, this topology is a good alternative to the six-switch buck type rectifier basically for transistor losses (Fig. 11 [14]) and also because, it is easier to control since it has just two high frequency transistors. Therefore, the Swiss Rectifier seems very promising in the research field of three-phase rectifiers.

The Swiss Rectifier is basically formed by a combination of two DC-DC buck converters and an active third harmonic

current injection. Replacing the buck converters by isolated converters, it is possible to provide the isolation in this power stage, hence a secondary isolated stage is not required anymore. The isolated converter could be either a Forward or Full-Bridge converter. In general, the Full-Bridge presents better performance in the range of several-kilowatt applications because it can reach ZVS and the voltage stress in the transistors is equal to the input voltage. On the other hand, the Forward converter has hard switching, and the voltage stress is higher than the input voltage. Nevertheless the Forward converter has just one power transistor leading to a less complex system.

Recent advances in semiconductor devices, especially silicon carbide devices (SiC), make it possible to find commercial high voltage transistors and diodes rated at 1200V and 1700V respectively. Despite of the high voltage, theses devices have excellent performances at high frequencies. This new technology has changed the design criteria in power electronics because topologies like the Forward converter with higher stresses in the devices are not highly penalized anymore and because of their simplicity now look more attractive.

In this work, a Forward topology was chosen over the Full-Bridge because of the simplicity and to take advantage of the new technology devices.

A. Principle of Operation

The principle of operation of the Swiss-Forward Rectifier is in its essence the same than that of the Swiss Rectifier [13], [14], the only difference being that the buck-type DC-DC converters are replaced by isolated forward-type DC-DC converters. Thus two transformers and the diodes D_+ and D_- are added in Fig. 2.

The diode bridge sets the voltage u_{PN} to the highest instantaneous voltage difference among the three input phases, while the bidirectional switches are used to control the remaining third phase. In this way, the voltages u_{PY} and u_{YN} are always positive and exhibit a quasi-triangular waveform, as shown in Fig. 3(c).

The main transistors T_P and T_N are controlled to generate a current proportional to the voltage in the positive and negative side of the diode-bridge. Assuming that the output DC-inductors work as constant current sources, the current through the transistors is proportional to the applied duty cycle as it can be seen in Fig. 3(d). In this way, the input current has a sinusoidal waveform proportional to the input capacitor voltages u_{Ca}, u_{Cb} and u_{Cc} in Fig. 3(b).

However the EMI filter generates an phase shift between the main voltages u_a, u_b and u_c and u_{Ca}, u_{Cb} and u_{Cc} in Fig. 3(a) preventing unitary power factor correction. This problem can be compensated adjusting the modulation.

B. Transformer Demagnetization

The transformers need to be demagnetized during operation, which can increase the voltage stress in the transistors T_P and T_N, depending on which demagnetizing method is used. In the rest of the components, i.e. the three-phase diode-bridge (D_{N+}, D_{N-}), the bidirectional switches (S_{y1}, S_{y2}, S_{y3}) and freewheeling diodes (D_{F+}, D_{F-}), the voltage stresses remain the same than in the Swiss Rectifier. Also the stresses in the input AC capacitors, output DC capacitors, the output inductors and EMI filters are equivalent to those of the Swiss
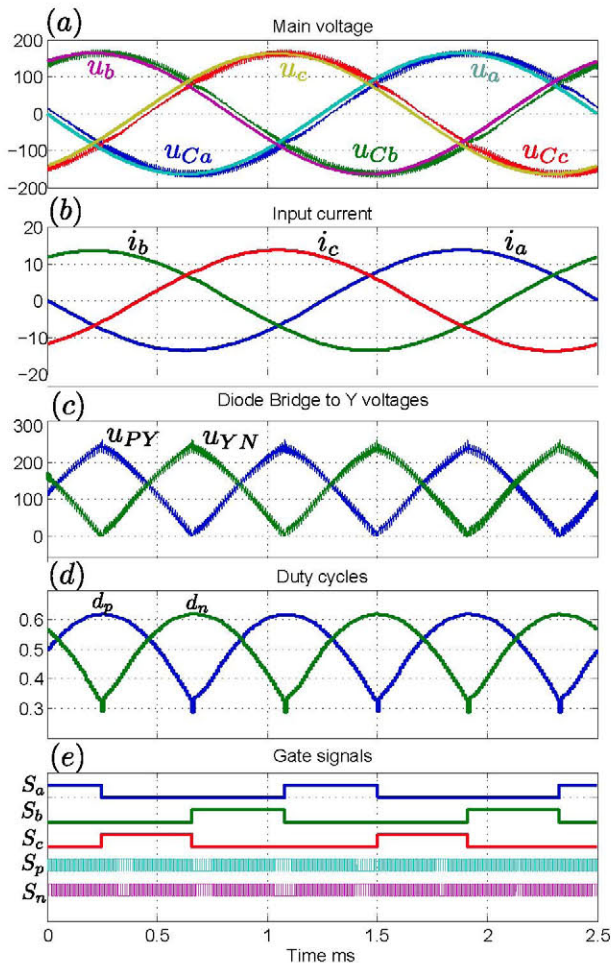
Figure 3. Main waveforms of the swiss-forward rectifier, (a)main voltages and input capacitor voltages. (b) input line currents, (c) diode bridge to Y node voltages, (d) duty cycles applied to the main transistors, (e) drive signals of all the transistors.
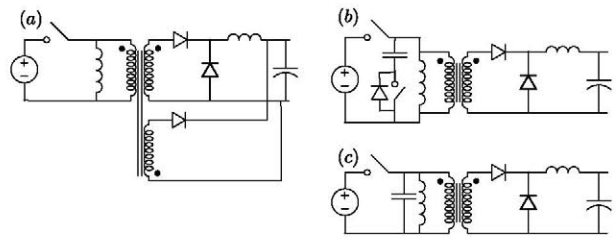

Figure 4. Forward topologies variation, depending on transformer demagnetization method: (a) forward-flyback converter, (b) active clamp PWM forward converter, (c) resonant reset forward converter.

Rectifier. In the following sections, the design criteria of the transformers are discussed as well as the transformer demagnetization circuit and the voltage stresses in the main transistors.

It is a well-known fact that the forward converter needs an extra energy path to demagnetize the transformer when the transistor is off. The most common technique is the use of an additional third winding in the transformer (Fig. 4(a)) to discharge the transformer through the input or the output [15], [16]. The disadvantage of this technique is the resulting more complex transformer as well as that the transformer can only work in a single quadrant of the magnetization curve. In the Swiss-Forward Rectifier the demagnetization through the input is not possible due to the diode-bridge which only allows unidirectional current flow. To use the output for demagnetization i.e forward-flyback topology, the output voltage needs to be above a specific threshold, a condition which is not fulfilled during the converter start-up phase, leading to potential problems.

The second most used technique for demagnetizing the transformer in the forward converter is the use of an active clamp (Fig. 4(b)) [17]–[19]. However the disadvantage of this

configuration is, that another transistor is necessary. Moreover this technique can only be easily used in a DC-DC forward converter. It is very important to note that, a significant difference with a DC-DC converter, the input voltage in the Forward-converter part of the Swiss-Forward converter is triangular, thus the voltage in the clamping capacitor has also a large ripple, preventing a proper demagnetization in all switching cycles.

A third technique to demagnetize the transformer is the resonant reset [20]–[22], which is very simple, in that it does not need an extra winding or any additional switch, but only one capacitor, however, the voltage stress in the transistor is higher than in the previous configurations. The voltage in the capacitor starts rising from zero, in this way the dynamics of the triangular input voltage does not affect the functionality of the reset circuit, thus it is an appropriate choice for use in the Swiss-Forward converter by using a high-voltage transistor.

Fig. 5 shows the principle of operation of the resonant reset network. During phase 1 the input voltage is applied to the transformer primary and the magnetizing current increases with a constant slope. In phase 2 the transistor is turned off, when the voltage in the capacitor reaches the input voltage, this capacitor starts to resonate with magnetizing inductance of the transformer, i.e. the inductance current decreases while the capacitor voltage increases. In phase 3 when the magnetizing current reaches zero the transistor voltage reaches the maximum and starts to decrease meanwhile the magnetizing current is negative. In phase 4, when the transistor voltage reaches the input voltage the diode D_1 is turned on, the secondary voltage is fixed to zero and the magnetizing current remains constant. In this way, regardless of the input voltage and the duty cycle (below a threshold), the capacitor voltage remains zero until the next period to restart at the same point. In spite of the fact that the transistors have to withstand the peak voltage, both the turn on and turn off take place at the input voltage which in the worst case is $3/2 \, \hat{U}_n$, in this manner the switching losses are not affected by the resonant circuit.

III. DESIGN CONSIDERATIONS IN THE SWISS-FORWARD RECTIFIER

As the Swiss-Forward Rectifier is a buck-type converter, the output voltage can be set from zero to a certain maximum level. However the turns ratio of the transformer allows to scale this maximum level, thus despite of the fact that this is a buck topology the output voltage can be set higher than the input voltage.
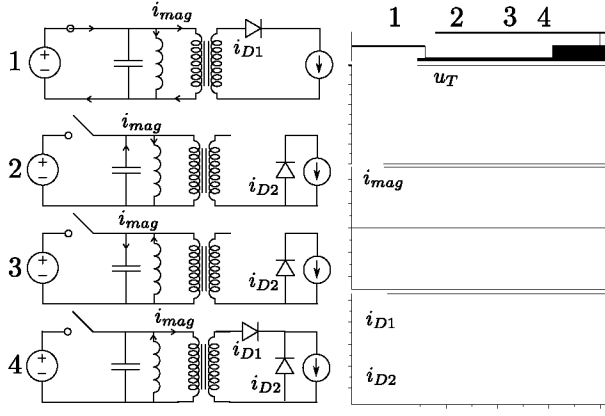
Figure 5. Equivalent circuit and main waveforms of the forward converter with resonant reset transformer demagnetization.

The output voltage is given by

$$u_{pn} = M \cdot \frac{N_2}{N_1} \cdot \frac{3}{2} \, \hat{U}_N \qquad (1)$$

where M is the modulation index, N_2/N_1 is the transformer turns ratio and $\hat{U}_N$ is the line to neutral voltage amplitude. Hence, in application requirements where both, the input and output voltage are fixed, the modulation index is not fixed because the turns ration provides an additional degree of freedom, unlike for the non-isolated topologies.

A. Stresses and Selection of Power Semiconductors

The transistors and diodes in this topology can be classified in two groups, those switching at low-frequency (twice the line-frequency) and those switching at high-frequency (switching frequency). The low-frequency devices are the three-phase diode-bridge (D_{N+} and D_{N-}) and the bidirectional switches of the active third-harmonic injection ($S_{y,123}$). The high-frequency devices are the Forward-transistors (T_P and T_N) and the secondary rectifier diodes (D_+, D_-, D_{F+} and D_{F-}).

The voltage stresses in the low-frequency devices are as follows: the voltage stress on the rectifier diodes is equal to the maximal line-to-line input voltage and the highest voltage stress on the bidirectional switches occurs at the moment when one line-voltage reaches its maximum amplitude while the other two are equal to minus half of their amplitude, resulting in the following equations:

$$\hat{u}_{DN+/-} = \sqrt{3} \cdot \hat{U}_N = \sqrt{3} \cdot \sqrt{2} \cdot 115V, \qquad (2)$$

$$\hat{u}_{Sy} = \frac{3}{2} \cdot \hat{U}_N = \frac{3}{2} \cdot \sqrt{2} \cdot 115V. \qquad (3)$$

The voltage stresses in the high-frequency diodes correspond to the voltage stresses in the low-frequency devices, multiplied by the turns-ratio of the transformer and are given by:

$$\hat{u}_D = \frac{N_2}{N_1} \cdot \hat{u}_{DN+/-}, \qquad (4)$$

$$\hat{u}_{DF} = \frac{N_2}{N_1} \cdot \hat{u}_{Sy}. \qquad (5)$$

None of the voltage stresses of the devices so far depend on the modulation index M. However, the higher M is, the shorter is the time that can be used to demagnetize the

transformer. This has a negative impact on the voltage stress in the transistors. The peak voltage in the transistors is given by the input voltage plus the peak voltage of the resonant circuit. The worst case scenario for this peak voltage is when the input voltage u_{PY} or u_{YN} is maximum ($\hat{U}_N$) and at the same time, the duty cycle is also the maximum ($d_n = M$ or $d_p = M$). Thus the maximum peak voltage is:

$$\hat{u}_T = \left(\frac{3\pi}{4} \cdot \frac{M}{1-M} + \frac{3}{2} \right) \hat{U}_N \qquad (6)$$

It can be seen in (6) that the voltage stress in the transistors increases with increasing modulation index M. A modulation index close to 1 would lead to very high voltage stress in the transistors, thus from the point of view of the transistor voltage stress, the modulation index should be selected to have a low value.

The RMS current $I_{T,RMS}$ of the two main transistors, depending on the modulation index M and the turns-ratio of the transformer, are defined as follows:

$$I_{T,avg} = I_{DC} \cdot \frac{N_2}{N_1} \cdot \frac{3M\sqrt{3}}{2\pi} \qquad (7)$$

$$I_{T,RMS} = I_{DC} \cdot \frac{N_2}{N_1} \cdot \sqrt{\frac{3M\sqrt{3}}{2\pi}} \qquad (8)$$

However these equations are not convenient in the design process, since the modulation index M and the turns-ratio are related through the converter input and output voltages, cf eq. (1). Rearranging (1) and substituting it in (7) and (8) provides us with the following, more design-oriented, equations:

$$I_{T,avg} = I_{DC} \cdot \frac{u_{pn}}{\hat{U}_N} \cdot \sqrt{3} \qquad (9)$$

$$I_{T,RMS} = I_{DC} \cdot \sqrt{\frac{2\sqrt{3}}{3\pi} \cdot \frac{u_{pn}}{\hat{U}_N} \cdot \frac{1}{\sqrt{M}}}, \qquad (10)$$

It can be seen in (9), that the average current through the transistors does not depend on the modulation index, but only on the DC-current and input-output voltage ratio. However the RMS current or the transistors is inversely proportional to the square-root of the modulation index. Therefore, from the point of view of the conduction losses in the transistors, the modulation index should be selected as high as possible.

The average and RMS currents through the high-frequency freewheeling and forward diodes are given by:

$$I_{DF,avg} = I_{DC} \left(1 - \frac{3\sqrt{3}}{2\pi} M \right) \qquad (11)$$

$$I_{DF,RMS} = I_{DC} \sqrt{1 - \frac{3\sqrt{3}}{2\pi} M} \qquad (12)$$

$$I_{DFor,avg} = I_{DC} \cdot M \frac{3\sqrt{3}}{2\pi} \qquad (13)$$

$$I_{DFor,RMS} = I_{DC} \cdot \sqrt{M \frac{3\sqrt{3}}{2\pi}} \qquad (14)$$

The average and RMS currents through the low-frequency three phase diode bridge and bidirectional switches are respectively given by:

$$I_{DN+/-,avg} = I_{DC} \cdot \frac{N_2}{N_1} \cdot M \cdot \frac{\sqrt{3}}{2\pi} \qquad (15)$$

Parameter	Value
Input line voltage	115Vrms
Main frequency	400Hz
Power Factor	98%
THD	5%
Switching frequency	100kHz
Output voltage	270V
Output current	12A
Output power rated	3.3kW
Semiconductor Voltage derating	75%

$$I_{DN+/-,RMS} = I_{DC} \cdot \frac{N_2}{N_1} \cdot \sqrt{\frac{\sqrt{3}M}{2\pi}} \quad (16)$$

$$I_{Sy,avg} = I_{DC} \cdot \frac{N_2}{N_1} \cdot M \cdot \frac{2-\sqrt{3}}{2\pi} \quad (17)$$

$$I_{Sy,RMS} = I_{DC} \cdot \frac{N_2}{N_1} \cdot \sqrt{M \cdot \frac{2-\sqrt{3}}{2\pi}} \quad (18)$$

B. Prototype Design Considerations

Table I shows the design specifications and requirements. In this application both the input and the output voltage are fixed, thus the product of M times N_1/N_2 is given by eq. (1). For a certain input and output voltage and I_{DC}, the higher M is, the lower is $I_{T,RMS}$. Fig 6(a) shows how $I_{T,RMS}$ changes for a M from 40% to 100%, as well as, the $I_{D+-,RMS}$ and $I_{DF+-,RMS}$.

On the other hand, Fig. 6(b) shows the peak transistor voltage for M from 40% to 80%. In order to design with the lowest possible transistor RMS current it is necessary to use a high voltage transistor. Currently due to advances in SiC devices, 1200V transistors can be used at high frequency with excellent performance such as the 1200V SiC JFET from Infineon or the 1200V SiC ZFET from Cree. With these transistors and considering a 75% voltage derating, the maximum possible M that can be used is 63%, getting a $I_{T,RMS}$ of 16A.

The bidirectional switches S_{y123} are implemented by two MOSFETs in series connected by their sources. These switches are implemented by an extreme low R_{on} transistor 650V/80A IPW65R037C6 which are optimized for low conduction losses, the switching losses are very low as they are switched only at twice the mains frequency (Fig. 3(e)).

The voltage stress in the diodes D_+ and D_- is the same than in the resonant capacitor, times the turns ratio of the transformer (1200V peak). To enable low switching losses, these diodes are implemented by 1700V Schottky SiC diodes C3D251704 from Cree. For D_{F+} and D_{F+} also SiC Schottky 600V diodes C3D20060D to achieve low switching losses. For the diodes D_{N+} and D_{N-}, as they do not switch at high frequency, ultra fast Si diodes STTH30R04 are used.

In table II all the main components are shown.

IV. CONTROL SCHEME

The control scheme of the Swiss-Forward Rectifier is shown in Fig. 7. The input line-to-line voltages are measured and fed into a digital PLL which provides the synchronized angle θ.
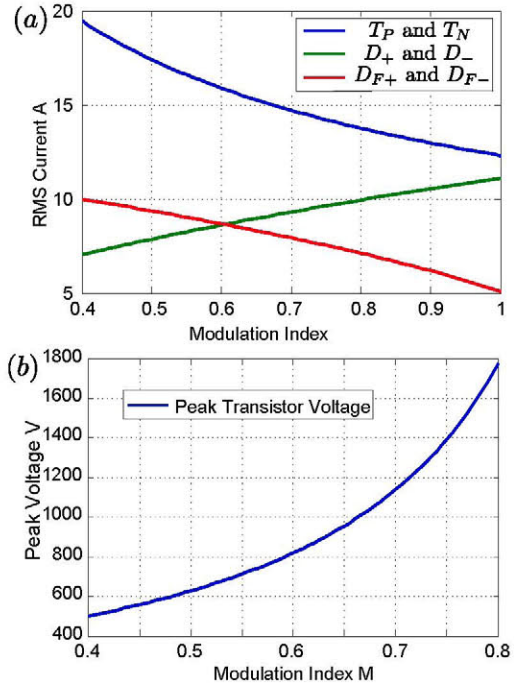
Figure 6. Current and voltage stresses in the main transistors: (a) $I_{T,RMS}$, D_{+-} and I_{F+-} as a function of the modulation index M, (b) peak voltage in the transistor as a function of the modulation index

System	Element	Description
EMI Filter	C_{1stage} L_{1stage}	3x0.56μF Murata X7T 450V 170μH, 3 stacked cores 58548 N= 21 4 parallel wires of 1mm diameter
	C_{2stage} L_{2stage}	6x0.56μF Murata X7T 450V 350μH, 2 stacked cores 58438 N= 38 4 parallel wires of 0.8mm diameter
Swiss Forward Rectifier	T_P and T_D D_+ and D_- D_{F+} and D_{F-} D_{N+} and D_{N-} $S_{y,123}$ Trafo L_{out} C_{out}	2xSiC C2M0080120D Power MOSFET C3D25170H Schottky diode SiC C4D30120D Schottky diode Si STTH30R04 Ultrafast recovery diode Si IPW65R037C6 CoolMOS ETD59, N1/N2 = 13/24, Litz wire 400x0.07mm. N2 3 parallel wire 2x150μH, core E65, gap 0.6mm, N87 9 parallel wire of 0.6mm 6x40μF F339M X2 450Vdc

Depending on the value of θ, the bidirectional switches are turned on or off. Then the minimal and maximal values of the three-phase sinusoidal signals are computed to generate the reference shape of the positive and negative three phase diode currents.

To control the output of the converter, a cascaded control system is used, consisting of two loops, one fast inner current control loop and a slower outer voltage control loop. The current regulator output corresponds to modulation index M. M is multiplied to the output of the current shaping blocks and theses values fed to the PWM modulator.

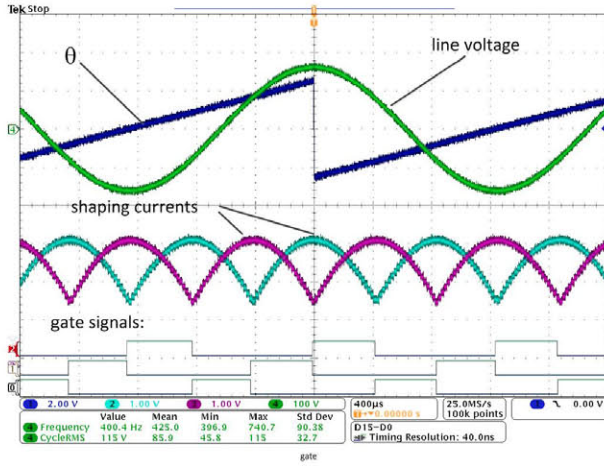The complete control and modulation schemes are imple-

Figure 7. Control scheme for Swiss-Forward Rectifier. Blue block corresponds to the logic implementation in the DSP, including the PWM peripherals (red bloks).

mented in a low cost floating point DSP, i.e. the TI F28069 control stick. It takes $16\mu s$ for the DSP to compute all the functions (PLL, PI controller, max and min functions, etc), thus the sampling frequency is conveniently set to 50kHz ($20\mu s$) and the duty cycle of both transistors is updated every two periods to reach the desired switching frequency of 100kHz.

To have access to all system signals inside the DSP, an external digital-to-analog converter (DAC AD5324) has been implemented. Using the serial-peripheral-interface (SPI) up to four signals are fed into the DAC and can be shown on the oscilloscope, which is very useful in the system debugging process.

V. EXPERIMENTAL WORK

A demonstrator converter prototype has been designed and has been built. The converter is designed for aircraft applications, i.e. three-phase input voltage with 115Vac and a grid frequency of 400Hz. The output voltage is 270Vdc and the converter is designed for a rated power of 3.3kW to comply with MIL STD-461 and -704, differential and common EMI filter are included. Fig. 8 shows the top and bottom views of the converter prototype and the main components are labeled.

The converter has been designed to be compact while allowing easy access to all key signals. The output capacitance is implemented using film capacitors because the converter requirements do not allow the use of electrolytic capacitors.

In Fig. 9 the voltage in phase A (green), and the angle θ (blue) are shown, as well as, shaping current signals (light blue and magenta) are shown from Fig 7, as well as the driving signals of the bidirectional switches. The DSP signals are shown through the DAC. The signal θ i.e. blue line, is perfectly

Figure 8. Developed three-phase 3.3kW 100kHz Isolated Swiss-Forward Rectifier 115Vac to 270Vdc hardware prototype using 1200V SiC MOSFETs, TI DSP controller F28069 Piccolo controlSTICK, including differential and common mode EMI filter.

Figure 9. DSP output signal. Channel 1 (blue), PLL output θ. Channel 2 (light blue), duty cycle of T_P. Channel 3 (red), duty cycle of T_N. Channel 4 (green), line to neutral voltage (v_{aN}). The digital signals show the drive signals to the bidirectional switches
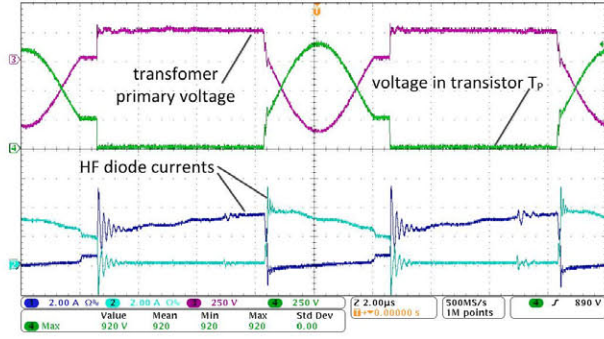

Figure 10. Resonance behavior between transformer and parasitic capacitances. Channel 1 (blue), forward diode current. Channel 2 (light blue), freewheeling current diode. Channel 3 (red), transformer primary voltage. Channel 4 (green), Drain source transistor voltage.

synchronized to the input voltage (green). Depending on the instantaneous value of θ, the bidirectional driving signals are set through three digital outputs of the DSP. Theses signals are shown in Fig 9 with digital channels of the oscilloscope. The duty cycles for T_P and T_N are shown in the light blue and magenta lines respectively. As it can be seen, in steady-state these waveforms correspond to the shaping currents multiplied by M an fed into the PWM blocks.

Fig. 10 shows the resonant voltage in the transistor T_P in the worst case when the $u_{PY} = 3/2 \cdot \hat{U}_N = 244V$. The peak transistor voltage is 920V while the aimed value is 900V. This peak can be reduced by adding more capacitance in the resonant circuit, however the size of this capacitance is in the order of hundreds of pF and is very difficult adjust perfectly. The blue and light blue lines show the high frequency diode currents. Meanwhile the resonance is happening D_{F+} is on and D_{F+} is off, when the resonance finishes, both diodes share the inductor current. When the transistor is turned on, unwanted current oscillations occur in D_{F+} due to parasitic capacitances of D_{F+}.

In Fig. 11, the steady state behavior of the input voltage (light blue) and current (magenta), as well as, the output voltage (blue) and DC inductor current (green) are shown
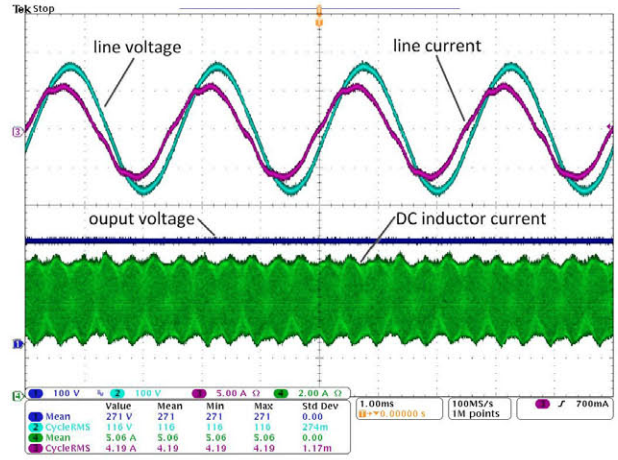

Figure 11. Steady state behavior of the input voltage (light blue) and current (red) and output voltage (blue) and DC inductor current (green)

at half of the nominal power (3.3kW). The THD in the input current is 4.5%, it is not lower because mainly of a distorsion generated when two line voltages reach the same value. However the current is still fully complying with the THD requirements. In addition, the input current and voltage are not in phase leading to a PF of 95%, this is because, the EMI filter generates a phase shift between the rectifier current and the grid current. By modifying the shaping current blocks it is possible to compensate the reactive power created in the EMI filter to obtain a perfectly synchronized voltage and current in the input. The output voltage i.e. blue line, is controlled to 270V and as can be seen, does not show any low frequency component which is a common problem in the control of three phase rectifiers. The DC inductor current (green) presents the envelope of the sixth harmonic of the mains frequency, however the upper and lower envelopes are compensated each other such that there is no low frequency component in this current either.

The results shown in Fig. 11 were performed at half of the nominal power. At higher power levels, the distortions in the input current are getting bigger, preventing compliance with the THD requirements. This problem is caused when two lines are at the same voltage, the voltage u_{PY} or u_{YN} is zero which are the input voltages of each forward. When this happens, the average current through T_P or T_N is not proportional to the respective duty cycle generating a disturbance in the system. Since the DC inductor current is bigger the voltage drop in the input capacitor is also bigger worsening this problem.

VI. CONCLUSIONS

This paper presented a new isolated, quasi-single-stage, three-phrase PWM rectifier topology based on the non-isolated Swiss Rectifier, denominated the Swiss-Forward Rectifier. The main principle of operation and the differences to the ordinary Swiss Rectifier have been discussed. A comparison of different demagnetization methods for the transformer has been performed and a prototype system has been built.

The solution presented in this work is a combination of an existing rectifier with an isolated Forward converter. Since this solution is a quasi-single stage topology, it allows to reduce the weight in comparison with a full two-stage configuration by

eliminating inductors and capacitors. A quasi single stage can also improve the efficiency, since the energy is not processed twice.

In this work, a Forward topology was chosen over the Full-Bridge because of the simplicity and to benefit of new technology SiC devices.

To minimize the RMS currents, a high modulation index is required, however, the higher the modulation index, the higher is the voltage across the main transistor. Considering a voltage derating of 75%, the maximum duty cycle applicable is 63%. However, if the system is designed to work in this point, the dynamic range for the duty cycle is limited avoiding a high dynamic response. A practical issue of adjusting the capacitance in the resonance is that the peak voltage transistor is highly dependent on the capacitor value as well as parasitic capacitances, which makes it difficult to adjust precisely.

The Swiss and Swiss-Forward Rectifiers, present problems when two lines have the same voltage creating low frequency distortions in the line current generating high THD. This problem depends on the relation between the input capacitance and the DC currents, because of the voltage ripple in the input capacitor. This problem can be attenuated by increasing the input capacitance, however this negatively affects the power factor of the rectifier.

The EMI filter generates a phase shift between the input current in the rectifier and the grid current. This phase shift depends on the output power. By modifying the current shaping blocks, it is possible to generate reactive power with the rectifier to decrease or even eliminate this phase shift.

REFERENCES

[1] R. D. Telford, S. Galloway, and G. M. Burt, "Evaluating the reliability amp; availability of more-electric aircraft power systems," in *Universities Power Engineering Conference (UPEC), 2012 47th International*, 2012, pp. 1–6.

[2] R. I. Jones, "The more electric aircraft: the past and the future?" in *Electrical Machines and Systems for the More Electric Aircraft (Ref. No. 1999/180), IEE Colloquium on*, 1999, pp. 1/1–1/4.

[3] B. Sarlioglu, "Advances in ac-dc power conversion topologies for more electric aircraft," in *Transportation Electrification Conference and Expo (ITEC), 2012 IEEE*, 2012, pp. 1–6.

[4] M. HARTMANN, "Ultra-compact and ultra-efficient three-phase pwm rectifier systems for more electric aircraft," Ph.D. dissertation, ETH Zurich, 2011.

[5] T. F. J. W. Kolar, "The essence of three-phase pfc rectifier systems," in *Proceedings of the 33rd IEEE International Telecommunications Energy Conference (INTELEC 2011), Amsterdam, Netherlands*, October 9-13 2011.

[6] G. Gong, U. Drofenik, and J. Kolar, "12-pulse rectifier for more electric aircraft applications," in *Industrial Technology, 2003 IEEE International Conference on*, vol. 2, 2003, pp. 1096–1101 Vol.2.

[7] G. Gong, M. L. Heldwein, U. Drofenik, J. Minibock, K. Mino, and J. W. Kolar, "Comparative evaluation of three-phase high-power-factor ac-dc converter concepts for application in future more electric aircraft," vol. 52, no. 3, pp. 727–737, 2005.

[8] M. Silva, N. Hensgens, J. Molina, M. Vasic, J. Oliver, P. Alou, O. Garcia, and J. Cobos, "Interleaved multi-cell isolated three-phase pwm rectifier system for aircraft applications," in *Applied Power Electronics Conference and Exposition (APEC), 2013 Twenty-Eighth Annual IEEE*, 2013, pp. 1035–1041.

[9] Y. Jang, M. M. Jovanovic, and J. M. Ruiz, "The single-stage taipei rectifier," in *Applied Power Electronics Conference and Exposition (APEC), 2013 Twenty-Eighth Annual IEEE*, 2013, pp. 1042–1049.

[10] Y. Jang and M. Jovanovic, "The taipei rectifier: A new three-phase two-switch zvs pfc dcm boost rectifier," *Power Electronics, IEEE Transactions on*, vol. 28, no. 2, pp. 686–694, 2013.

[11] V. Vlatkovic, D. Borojevic, and F. Lee, "A zero-voltage switched, three-phase isolated pwm buck rectifier," *Power Electronics, IEEE Transactions on*, vol. 10, no. 2, pp. 148–157, 1995.

[12] J. Kolar, U. Drofenik, and F. C. Zach, "Vienna rectifier ii-a novel single-stage high-frequency isolated three-phase pwm rectifier system," *Industrial Electronics, IEEE Transactions on*, vol. 46, no. 4, pp. 674–691, 1999.

[13] T. Soeiro, T. Friedli, and J. Kolar, "Swiss rectifier: A novel three-phase buck-type pfc topology for electric vehicle battery charging," in *Applied Power Electronics Conference and Exposition (APEC), 2012 Twenty-Seventh Annual IEEE*, 2012, pp. 2617–2624.

[14] ——, "Three-phase high power factor mains interface concepts for electric vehicle battery charging systems," in *Applied Power Electronics Conference and Exposition (APEC), 2012 Twenty-Seventh Annual IEEE*, 2012, pp. 2603–2610.

[15] J. Sebastian, J. Uceda, M. Rico, M. Perez, and F. Aldana, "A complete study of the double forward-flyback converter," in *Power Electronics Specialists Conference, 1988. PESC '88 Record., 19th Annual IEEE*, 1988, pp. 142–149 vol.1.

[16] M. Vazquez, E. de la Cruz, J. Navas, and J. Cobos, "Fixed frequency forward-flyback converter with two fully regulated outputs," in *Telecommunications Energy Conference, 1995. INTELEC '95., 17th International*, 1995, pp. 161–166.

[17] J. Cobos, O. Garcia, J. Sebastian, and J. Uceda, "Active clamp pwm forward converter with self driven synchronous rectification," in *Telecommunications Energy Conference, INTELEC '93. 15th International*, vol. 2, 1993, pp. 200–206 vol.2.

[18] B.-R. Lin, H.-K. Chiang, C.-E. Huang, and D. Wang, "Analysis, design and implementation of an active clamp forward converter with synchronous rectifier," in *TENCON 2005 2005 IEEE Region 10*, 2005, pp. 1–6.

[19] K.-W. Lee, S.-W. Choi, B.-H. Lee, and G.-W. Moon, "Current boosted active clamp forward converter without output filter," in *Energy Conversion Congress and Exposition, 2009. ECCE 2009. IEEE*, 2009, pp. 2873–2880.

[20] J. Cobos, O. Garcia, J. Sebastian, and J. Uceda, "Resonant reset forward topologies for low output voltage on board converters," in *Applied Power Electronics Conference and Exposition, 1994. APEC '94. Conference Proceedings 1994., Ninth Annual*, 1994, pp. 703–708 vol.2.

[21] P. Alou, J. Cobos, O. Garcia, R. Prieto, and J. Uceda, "Design guidelines for a resonant reset forward converter with self-driven synchronous rectification," in *Industrial Electronics, Control and Instrumentation, 1997. IECON 97. 23rd International Conference on*, vol. 2, 1997, pp. 593–598 vol.2.

[22] X. Xie, J. Zhang, G. Luo, D. Jiao, and Z. Qian, "An improved self-driven synchronous rectification for a resonant reset forward converter," in *Applied Power Electronics Conference and Exposition, 2003. APEC '03. Eighteenth Annual IEEE*, vol. 1, 2003, pp. 348–351 vol.1.